Polymer 54 (2013) 6516–6525

Contents lists available at ScienceDirect

Polymer

journal homepage: www.elsevier.com/locate/polymer

Synthesis and properties of hydroxylated core-fluorinated diamines and polyurethanes based on them with azobenzene nonlinear optical chromophores in the backbone

V.V. Shevchenko [a,*], A.V. Sidorenko [a], V.N. Bliznyuk [b], I.M. Tkachenko [a], O.V. Shekera [a], N.N. Smirnov [c], I.A. Maslyanitsyn [d], V.D. Shigorin [d], A.V. Yakimansky [c], V.V. Tsukruk [e]

[a] Institute of Macromolecular Chemistry of the National Academy of Sciences of Ukraine, 48 Kharkivske shosse, Kiev 02160, Ukraine
[b] Department of Materials Science and Engineering, Clemson University, Clemson, SC 29634, USA
[c] Institute of Macromolecular Compounds of the Russian Academy of Sciences, Bolshoi pr. 31, St. Petersburg 199004, Russia
[d] Prokhorov Institute of General Physics of the Russian Academy of Sciences, ul. Vavilova 38, Moscow 119991, Russia
[e] School of Materials Science and Engineering, Georgia Institute of Technology, Atlanta, GA 30332-0245, USA

ARTICLE INFO

Article history:
Received 15 August 2013
Received in revised form
24 September 2013
Accepted 25 September 2013
Available online 8 October 2013

Keywords:
Fluorinated azo-polyurethanes
Azo-chromophores
Second harmonic generation (SHG)

ABSTRACT

We report on the synthesis of core-fluorinated phenylene- and biphenyldianilines, which was accomplished by diazotization reaction of diamines followed by coupling of the obtained diazonium salts with 2-[ethyl(phenyl)amino]-ethanol. Two types of core-fluorinated aromatic units were used in a molecular design of azo-chromophore monomers with enhanced second order nonlinear optical (NLO) properties: octafluorobiphenyl (OFB) and tetrafluorobenzene (TFB) ones. Polymerization of the monomers was performed to obtain polyurethanes with azo-chromophores in the main chain. Comparison of physical and optical properties of these polymers reveals that the main factor influencing the observed NLO activity of the latter is the inherent isomery of the macromolecular chains rather than a variation of the structure of electron-accepting groups.

1. Introduction

Polyurethanes (PU) containing azobenzene chromophore groups represent an interesting class of nonlinear optical (NLO) polymers [1,2]. Such azo-polyurethenes (APU) have an advantage over other polymers with chromophores like azomethine or methine groups in their optical second harmonic generation coefficients [1–3]. They are also characterized with an enhanced radiation stability, high optical nonlinearity and transparency, low dielectric constant. Relative simplicity of their synthesis, post-treatment and modification makes such polymer materials an attractive alternative to traditional inorganic systems [2–7]. High glass transition temperature prevents fast dipole relaxation of the chromophore fragments at elevated temperatures. Therefore, the APUs are promising systems for creation of polymer NLO media with enhanced time and temperature stability [8–10].

Azo-chromophore groups can be introduced into the polymer chain in two different ways: as side groups or as a part of the backbone. Moreover, the way of their attachment will influence the final NLO properties of such polymers [1,2]. APUs with side chain chromophores have better chances to be aligned by an external electric field (poling process) to obtain an asymmetric arrangement of chromophore groups required for the second order nonlinearity. On the contrary, APU with the same chromophores incorporated in the backbone typically have a developed network of intermolecular hydrogen bonds, leading to higher T_g and higher time and temperature stability of their NLO properties [8,11,12].

The same initial bifunctional hydroxyl-containing azomonomer compounds (like bis-diols and bis-phenols) can be used both for the synthesis of side chain [3,9,13–15] and main chain polyurethanes [16–22]. A common feature for the monomers of this type is their D–π–A structure, where donor (D) and acceptor (A) groups are covalently bound to opposite ends of a fragment with extended π-electron conjugation [1–3,23–25]. One of a typical monomer of such kind is a chromophore Disperse Red-19 (DR-19, 2,2′-({4-[(*E*)-(4-Nitrophenyl) diazenyl] phenyl}imino)diethanol)) and its derivatives. There are also some reports on application of chromophores with more complex architecture: $(D)_2$–π–A (Y or T type chromophores) [9–11,26,27],

* Corresponding author. Tel.: +380 44 559 5500; fax: +380 44 292 4064.
E-mail addresses: valshevchenko@yandex.ru, valery_petr@i.ua (V.V. Shevchenko), yak@hq.macro.ru (A.V. Yakimansky), vladimir@mse.gatech.edu (V.V. Tsukruk).

0032-3861/$ – see front matter © 2013 Elsevier Ltd. All rights reserved.
http://dx.doi.org/10.1016/j.polymer.2013.09.053

$(D)_2$–π–$(A)_2$ (Ч-type chromophores) [28], and D–π–A–π–D (V-type chromophores) [29].

A natural way of preparation of APUs with enhanced NLO properties is usage of monomers with high values of β for their synthesis. The molecular design of such compounds is based on optimization of the electron structure of chromophores via variation of electron-donor and electron-acceptor substituents [30–35], changing a position of functional groups [32], or extension of the conjugated structure [3,36]. However, this strategy comes across some obstacles. They are, first of all, related to a strong coupling between neighboring polar chromophore groups. As a result, an asymmetric orientation imposed by the poling process of chromophores is unstable and has a trend to relax towards a more stable symmetric arrangement, deteriorating the NLO properties of the polymer material [7,37].

To control intermolecular interactions between chromophores and to preserve their asymmetric orientation, the spatial architecture of APU has to be adjusted without changes in their electronic configuration. This can be accomplished, for instance, via incorporation of additional chemical groups in order to screen the interaction between neighboring chromophores (so-called suitable isolation groups or SIG groups) [30,38–40]. As an additional advantage of such approach, the SIG groups provide an opportunity to tune up finely the NLO properties of APU via a special choice of their chemistry as well as of their chemical attachment within the PU monomer.

We have developed an approach to the synthesis of azo-containing monomers of various nature based on electron-acceptor core-fluorinated phenyl or biphenyl fragments with different isomery of substituting groups. Application of such monomers for the synthesis of PU makes it possible to prepare polymers with optical and NLO characteristics depending on the isomer type. Due to their chemical composition (presence of fluorinated phenyl rings with extended conjugation), these new polymers are expected to have also enhanced thermal stability and useful optical properties (reduced refractive index and optical losses). Because of a strong influence of the type of isomer fragments on the structure and properties of polymer materials, one can expect an asymmetric arrangement of chromophores required for the system to possess NLO properties. In other words, one can expect that the isomeric configuration of the chromophore will play a role similar to that of SIG's group with its possible accomplishment at the macromolecular level.

Therefore, the aim of this study was to synthesize new monomers having isomer core-fluorinated azo-fragments of V-type (with D–π–A–π–D electron configuration) as well as to investigate the structure and NLO properties of polymers based on them, depending on the isomer configuration of the NLO chromophore.

2. Experimental

2.1. Materials

2-[ethyl(phenyl)amino] ethanol (96%, "Acros Organics"), $NaNO_2$, HCl (36%), Na_2CO_3 and NaCl were received from different commercial sources and used without further purification. 4,4′-Methylenebis(phenyl isocyanate) (MDI) (99%, "Aldrich"), N,N-Dimethylformamide (DMF) (99%, "Aldrich") were purified by distillation under reduced pressure before use.

2.2. Monomers

4,4′-[(2,3,5,6-tetrafluoro-1,4-phenylene)-bis-(oxy)]dianiline (**DA-I**), 3,3′-[(2,3,5,6-tetrafluoro-1,4-phenylene)-bis-(oxy)]dianiline (**DA-II**), 2,2′-[(2,3,5,6-tetrafluoro-1,4-phenylene)-bis-(oxy)]dianiline (**DA-III**), 4,4′-[(2,2′,3,3′,5,5′,6,6′-octafluorobiphenyl-4,4′-diyl)bis(oxy)]dianiline (**DA-IV**), 3,3′-[(2,2′,3,3′,5,5′,6,6′-octafluorobiphenyl-4,4′-diyl)bis(oxy)]dianiline (**DA-V**) и 2,2′-[(2,2′,3,3′,5,5′,6,6′-octafluorobiphenyl-4,4′-diyl)bis(oxy)]dianiline (**DA-VI**) were synthesized according to [41].

2.3. Synthesis of diamines (*GDA-I*–*GDA-VI*)

2.3.1. 2,2′-{(2,3,5,6-tetrafluoro-1,4-phenylene)bis[oxy-1,4-phenylene(E)diazene-1,2-diyl-1,4-phenylene(ethylimino)]}diethanol (*GDA-I*)

A solution of sodium nitrite (5.5 mmol) in 2.2 ml water was added dropwise with stirring to a cooled solution of 4,4′-[(2,3,5,6-tetrafluoro-1,4-phenylene)-bis-(oxy)]dianiline (DA-I) (1.0 g, 2.7 mmol) dissolved in 3.0 ml concentrated hydrochloric acid 18% (16.5 mmol) at a temperature between 0 and 5 °C for 2 h. The resulting diazonium salt was coupled with 2-[ethyl(phenyl)amino] ethanol (0.91 g, 5.5 mmol) dissolved in 5.8 ml hydrochloric acid 1.8% at a temperature between 0 and 5 °C over 2 h. Then sodium acetate was added, the solution was left in an ice bath for 1 h, additional sodium acetate was added, and the reaction mixture was left for 30 min. After the temperature increased to room temperature, sodium hydroxide solution was added until the pH of the solution reached 6 and the mixture was stirred at room temperature for 1 h. The obtained monomer was washed with water and recrystallized from ethanol. This general procedure was used for all the obtained diamines. Yield: 0.71 g (65%). Melting point (m.p): 180–183 °C. ^{1}H NMR (DMSO-d_6): 7.82 ppm (d, 4H, J = 8.82 Hz, Ar–H), 7.78 ppm (d, 4H, J = 8.82 Hz, Ar–H), 7.4 ppm (d, 4H, J = 8.82 Hz, Ar–H), 6.84 ppm (d, 4H, J = 8.82 Hz, Ar–H), 4.83 ppm (t, 2H, J = 4.67, OH), 3.61 ppm (q, 4H, J = 4.67, CH_2), 3.5 ppm (m, 8H, CH_2), 1.15 ppm (t, 6H, J = 6.75 Hz, CH_3). ^{19}F NMR: −156.65 ppm (s, 4F, Ar–F). IR (KBr): 3371 cm^{-1} (OH), 3072 cm^{-1} (C–H), 2966 cm^{-1} (CH_3), 2926 cm^{-1} (CH_2), 2872 cm^{-1} (CH_3), 1392 cm^{-1} (CH), 1601, 1512, 1489 cm^{-1} (Ar), 1005, 991 cm^{-1} (C–F). UV–vis: λ_{max} = 432 nm.

2.3.2. 2,2′-{(2,3,5,6-tetrafluoro-1,4-phenylene)bis[oxy-1,3-phenylene(E)diazene-1,2-diyl-1,4-phenylene(ethylimino)]}diethanol (*GDA-II*)

Yield 85%. Melting point (m.p): 185–188 °C. ^{1}H NMR (DMSO-d_6): 7.78 ppm (d, 4H, J = 7.33 Hz, Ar–H), 7.59–7.55 ppm (m, 6H, Ar–H), 7.29 ppm (s, 2H, Ar–H), 6.84 ppm (d, 4H, J = 6.36 Hz, Ar–H), 4.79 (s, 2H, OH), 3.61 (s, 4H, CH_2), 3.51 (m, 8H, CH_2), 1.16 (s, 6H, CH_3). ^{19}F NMR: −155.56 ppm (s, 4F, Ar–F). IR (KBr): 3292 cm^{-1} (OH), 3067 cm^{-1} (C–H), 2965 cm^{-1} (CH_3), 2924 cm^{-1} (CH_2), 2870 cm^{-1} (CH_3), 2854 cm^{-1} (CH_2), 1394 cm^{-1} (CH), 1601, 1512, 1499 cm^{-1} (Ar), 1018, 993 cm^{-1} (C–F). UV–vis: λ_{max} = 440 nm.

2.3.3. 2,2′-{(2,3,5,6-tetrafluoro-1,4-phenylene)bis[oxy-1,2-phenylene(E)diazene-1,2-diyl-1,4-phenylene(ethylimino)]}diethanol (*GDA-III*)

Yield 82%. Melting point (m.p): 147–150 °C. ^{1}H NMR (DMSO-d_6): 7.58 ppm (m, 6H, Ar–H), 7.34 ppm (t, 2H, J = 6.36 Hz, Ar–H), 7.26 (t, 2H, J = 6.85 Hz, Ar–H), 7.15 ppm (d, 2H, J = 6.36 Hz, Ar–H), 6.74 ppm (d, 4H, J = 5.38 Hz, Ar–H), 4.83 ppm (s, 2H, OH), 3.58 ppm (s, 4H, CH_2), 3.47 ppm (m, 8H, CH_2), 1.11 ppm (s, 6H, CH_3). ^{19}F NMR: −156.78 ppm (s, 4F, Ar–F). IR (KBr): 3393 cm^{-1} (OH), 3072 cm^{-1} (C–H), 2972 cm^{-1} (CH_3), 2926 cm^{-1} (CH_2), 2874 cm^{-1} (CH_3), 1394 cm^{-1} (CH), 1600, 1512, 1501 cm^{-1} (Ph), 1003, 995 cm^{-1} (C–F). UV–vis: λ_{max} = 442 nm.

2.3.4. 2-[ethyl(4-{(E)-[4-({4′-[4-((E)-{4-[ethyl(propyl)amino]phenyl}diazenyl)phenoxy]-2,2′,3,3′,5,5′,6,6′-octafluorobiphenyl-4-yl}oxy)phenyl]diazenyl}phenyl)amino]ethanol (*GDA-IV*)

Yield 74%. Melting point (m.p): 169–171 °C. ^{1}H NMR (DMSO-d_6): 7.83 ppm (d, 4H, J = 8.31 Hz, Ar–H), 7.77 ppm (d, 4H, J = 8.31 Hz,

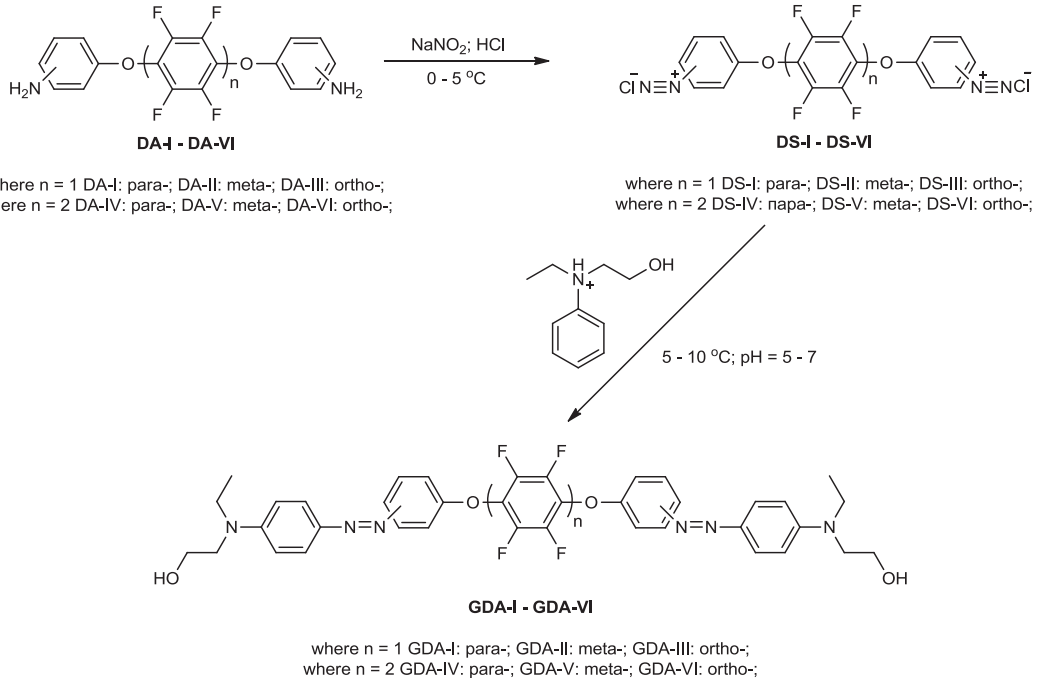

Fig. 1. Synthetic route and chemical structure of core-fluorinated diamines containing main azobenzene groups.

Ar–H), 7.41 ppm (d, 4H, J = 8.8 Hz, Ar–H), 6.84 ppm (d, 4H, J = 8.8 Hz, Ar–H), 4.83 ppm (t, 2H, J = 4.89 Hz, OH), 3.61 ppm (q, 4H, J = 4.9 Hz, CH_2), 3.5 ppm (m, 8H, CH_2), 1.15 ppm (t, 6H, J = 6.85 Hz, CH_3). ^{19}F NMR: −136.53 ppm (d, 4F, Ar–F), −153.73 ppm (d, 4F, Ar–F). IR (KBr): 3383 cm^{-1} (OH), 3072, cm^{-1} (C–H), 2972 cm^{-1} (CH_3), 2930 cm^{-1} (CH_2), 2876 cm^{-1} (CH_3), 1394 cm^{-1} (CH), 1599, 1514, 1487 cm^{-1} (Ph), 1003, 980 cm^{-1} (C–F). UV–vis: λ_{max} = 418 nm.

2.3.5. 2-[ethyl(4-{(E)-[3-({4′-[3-((E)-{4-[ethyl(propyl)amino]phenyl}diazenyl)phenoxy]-2,2′,3,3′,5,5′,6,6′-octafluorobiphenyl-4-yl}oxy)phenyl]diazenyl}phenyl)amino]ethanol (*GDA-V*)

Yield 93%. Melting point (m.p): 174–177 °C. ^{1}H NMR (DMSO-d_6): 7.77 ppm (d, 4H, J = 5.87 Hz, Ar–H), 7.62–7.57 ppm (m, 6H, Ar–H), 7.32 (s, 2H, J, Ar–H), 6.84 ppm (d, 4H, J = 6.84 Hz, Ar–H), 4.83 ppm (s, 2H, OH), 3.6 ppm (s, 4H, CH_2), 3.5 ppm (s, 8H, CH_2), 1.15 ppm (s, 6H, CH_3). ^{19}F NMR: −137.46 ppm (d, 4F, Ar–F), −153.11 ppm (d, 4F, Ar–F). IR (KBr): 3400 cm^{-1} (OH), 3071 cm^{-1} (C–H), 2957 cm^{-1} (CH_3), 2928 cm^{-1} (CH_2), 2874 cm^{-1} (CH_3), 1396 cm^{-1} (CH), 1599, 1514, 1489 cm^{-1} (Ph), 1001, 980 cm^{-1} (C–F). UV–vis: λ_{max} = 426 nm.

2.3.6. 2-[ethyl(4-{(E)-[2-({4′-[2-((E)-{4-[ethyl(propyl)amino]phenyl}diazenyl)phenoxy]-2,2′,3,3′,5,5′,6,6′-octafluorobiphenyl-4-yl}oxy)phenyl]diazenyl}phenyl)amino]ethanol (*GDA-VI*)

Yield 84%. Melting point (m.p): 145–148 °C. ^{1}H NMR (DMSO-d_6): 7.58 ppm (m, 6H, Ar–H), 7.35 ppm (t, 2H, J = 7.34 Hz, Ar–H), 7.26 ppm (t, 2H, J = 7.34 Hz, Ar–H), 7.16 ppm (d, 2H, J = 6.36 Hz, Ar–H), 6.74 ppm (d, 4H, J = 5.87 Hz, Ar–H), 4.82 ppm (s, 2H, OH), 3.58 ppm (s, 4H, CH_2), 3.47 ppm (m, 8H, CH_2), 1.11 ppm (s, 6H, CH_3). ^{19}F NMR: −136.74 ppm (d, 4F, Ar–F), −151.31 ppm (d, 4F, Ar–F). IR (KBr): 3390 cm^{-1} (OH), 3072 cm^{-1} (C–H), 2970 cm^{-1} (CH_3), 2928 cm^{-1} (CH_2), 2874 cm^{-1} (CH_3), 1394 cm^{-1} (CH), 1599, 1516, 1489 cm^{-1} (Ph), 1001, 982 cm^{-1} (C–F). UV–vis: λ_{max} = 434 nm.

2.4. Polymer synthesis

APU-I to **APU-VI** polymers were synthesized by the reaction of equimolar ratios of the corresponding hydroxyethylated diamine (**GDA-I**–**GDA-VI**) with MDI under an inert atmosphere with vigorous stirring for 24 h in DMF at 120 °C. The concentration of the reactants was 15%. After completion the reaction, the reaction mixture was precipitated into methanol. The resulting product was filtered and washed with water.

APU-I. 0.2 g (0.28 mmol) **GDA-I**, 0.07 g MDI (0.28 mmol). Yield 0.22 g (81%). IR (KBr): 3317 cm^{-1} (NH), 2923, 2853, cm^{-1} (C–H), 1705 cm^{-1} (COO), 1670, 1232 cm^{-1} (C–O–C).

APU-II. 0.2 g (0.28 mmol) **GDA-II**, 0.07 g MDI (0.28 mmol). Yield 0.24 g (90%). IR (KBr): 3400 cm^{-1} (NH), 2926 cm^{-1} (C–H), 1730, 1713 cm^{-1} (COO), 1659, 1229 cm^{-1} (C–O–C).

APU-III. 0.2 g (0.28 mmol) **GDA-III**, 0.07 g MDI (0.28 mmol). Yield 0.21 g (80%). IR (KBr): 3331 cm^{-1} (NH), 2931, 2857 cm^{-1} (C–H), 1732 cm^{-1} (COO), 1652, 1539, cm^{-1} (C=O), 1223 cm^{-1} (C–O–C).

APU-IV. 0.2 g (0.23 mmol) **GDA-IV**, 0.058 g MDI (0.23 mmol). Yield 0.2 g (80%). IR (KBr): 3325 cm^{-1} (NH), 2935, 2858, 2797 cm^{-1} (C–H), 1728 cm^{-1} (COO), 1647, 1585 cm^{-1} (C=O), 1245 cm^{-1} (C–O–C).

APU-V. 0.2 g (0.23 mmol) **GDA-V**, 0.058 g MDI (0.23 mmol). Yield 0.24 g (95%). IR (KBr): 3305 cm^{-1} (NH), 2939, 2920, 2851, 2797 cm^{-1} (C–H), 1728 cm^{-1} (COO), 1643, 1539 cm^{-1} (C=O), 1230 cm^{-1} (C–O–C).

APU-VI. 0.2 g (0.23 mmol) **GDA-VI** and 0.058 g MDI (0.23 mmol). Yield 0.2 g (75%). IR (KBr): 3306 cm^{-1} (NH), 2939, 2958, 2797 cm^{-1} (C–H), 1728, 1705 cm^{-1} (COO), 1647, 1535 cm^{-1} (C=O), 1222 cm^{-1} (C–O–C).

2.5. Instrumentation

^{1}H and ^{19}F NMR spectra were recorded using a Bruker Avance DRX 500 spectrometer with tetramethylsilane (TMS) and $CFCl_3$ as internal standards, respectively. UV spectra were recorded with a Specord 210 (Analytikjena) spectrometer using DMF solutions of compounds. Fourier-transform infrared (FT-IR) spectra were studied in the range of 400–4000 cm^{-1} using a “TENSOR 37” spectrometer and polymer samples pressed in KBr pellets.

Glass transition temperatures of the polymers under study were determined, using an Q-2000 TA Instruments (USA) differential

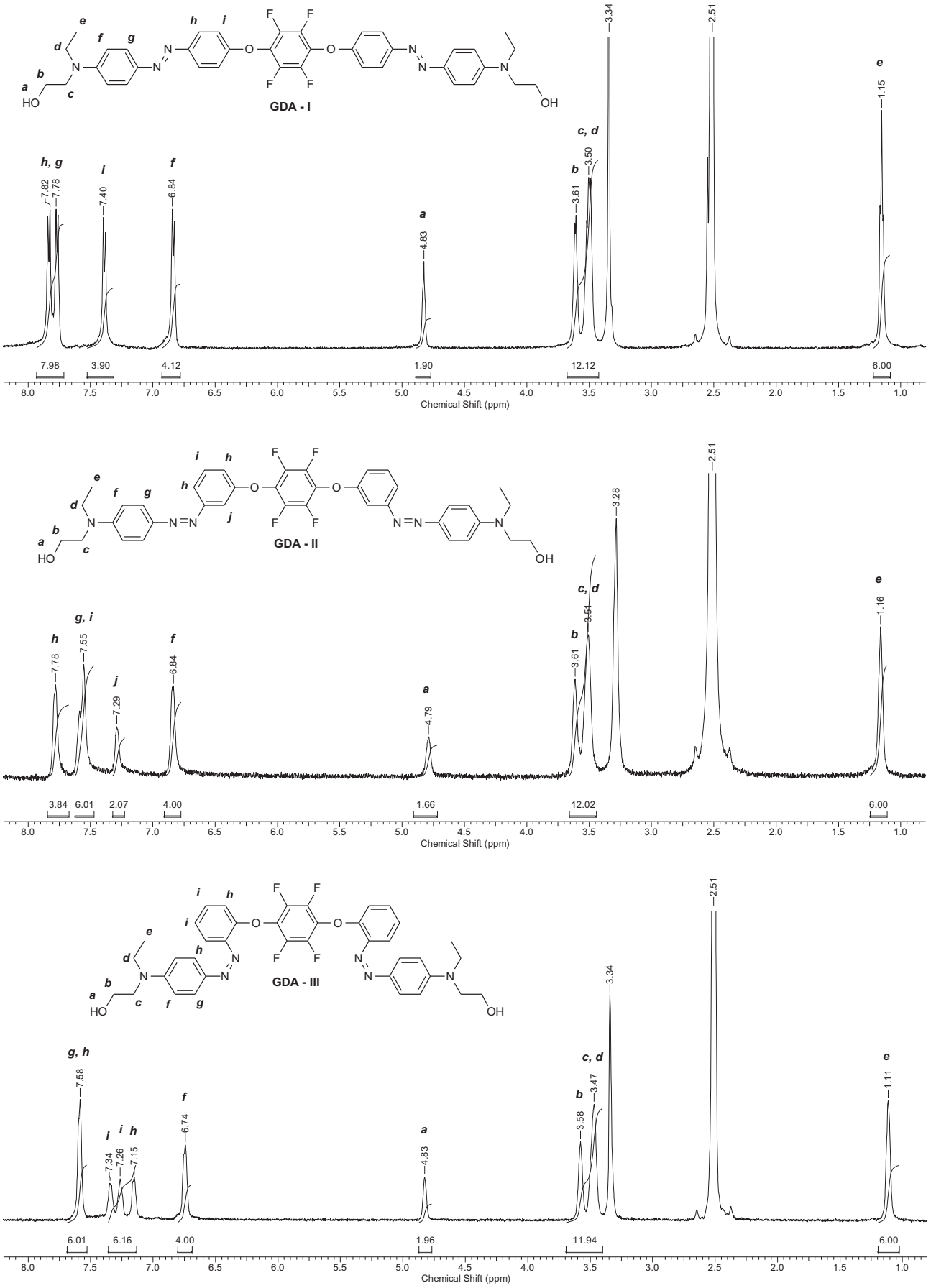

Fig. 2. ^{1}H NMR spectra of the core-fluorinated **GDA-I - GDA-VI**.

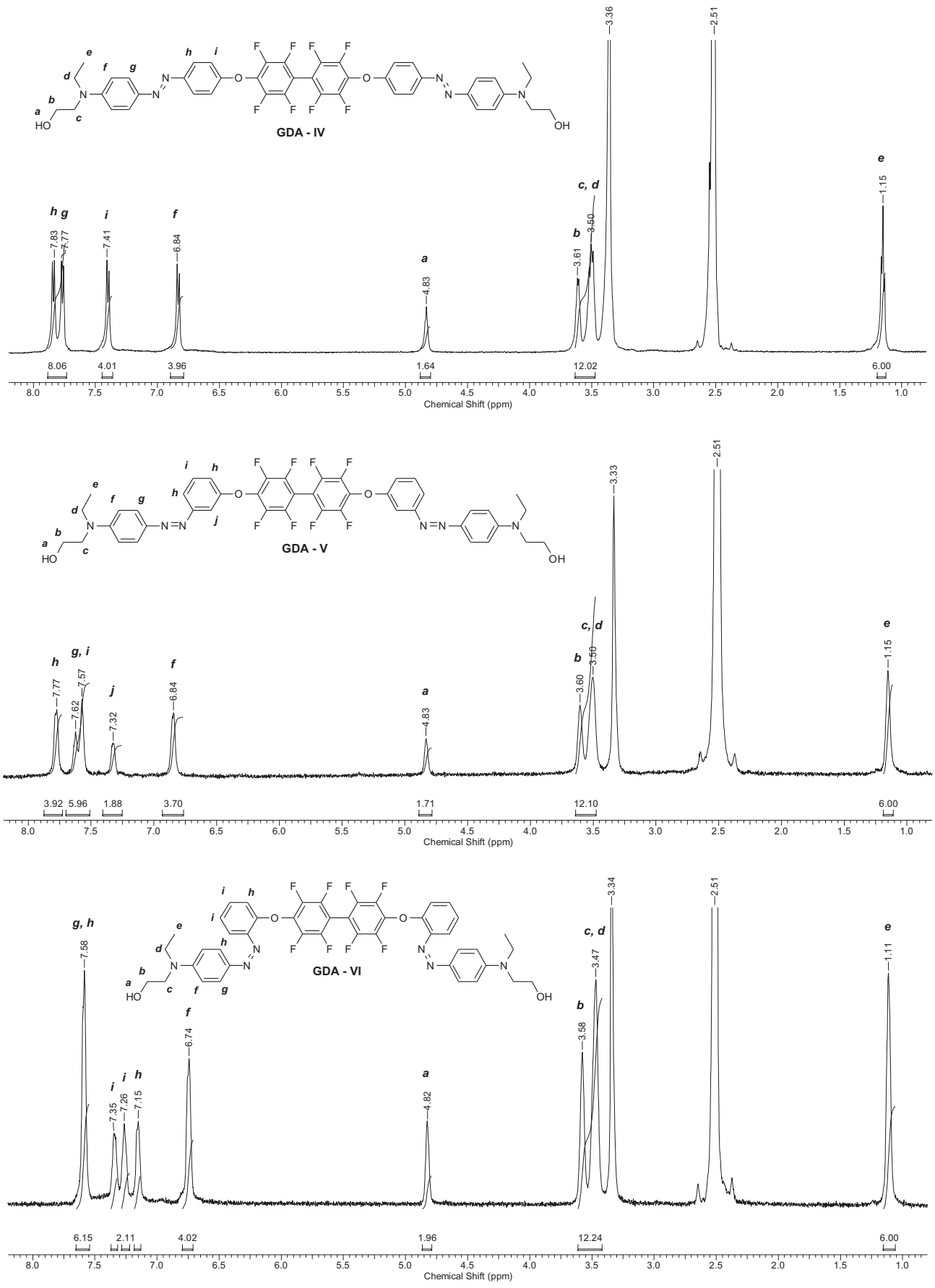

Fig. 2. (*continued*).

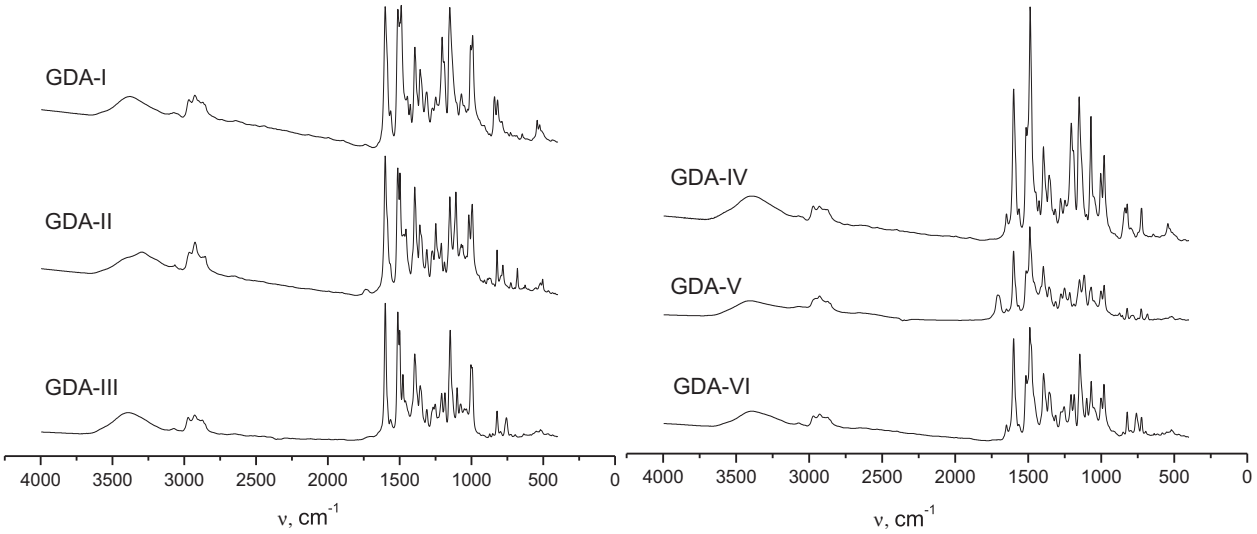

Fig. 3. IR spectra of core-fluorinated **GDA-I**–**GDA-VI** compounds.

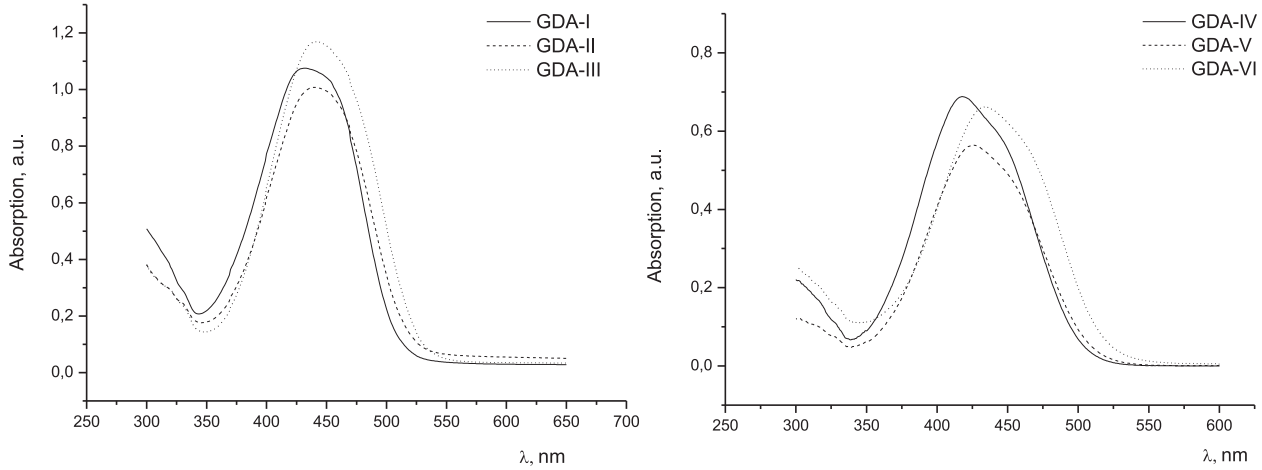

Fig. 4. UV-vis spectra of core fluorinated **GDA-I**–**GDA-VI** compounds.

scanning calorimetry (DSC) equipment. The rate of heating was 20 °C^{-1}. Thermal stability of the samples was studied by thermogravimetric analysis (TGA). For this aim, a Du Pont instrument 951TGA was applied with a heating rate 20 °C^{-1} on air. A Woolam M2000U spectroscopic multi-angle ellipsometer coupled with a WVASE32 modeling software was applied to characterize optical constants of the samples in the range of wavelengths from 245 to 1000 nm under three incidence angles 65, 70, and 75°. The effective thickness of samples was estimated using a multilayer model with a SiO_2 glass substrate by an independent fit of three sample parameters: the refractive index (n), the absorption coefficient (k), and the film thickness. The fitting procedure was repeated for each of three used incident angles.

NLO properties of the polymers under study were measured for thin spin-coated films with the thickness d in the range of 0.17–0.62 μm as measured with ellipsometry (Woolam M2000). The films were obtained from polymer solutions (5–10% in DMFA) using a rotation speed of 600–3000 rpm. The samples were dried for 8 h on air at 50–70 °C and then for 4 h in vacuum at 120 °C after their deposition by spin-coating.

Poling of the samples was accomplished with a homemade corona discharge device under application of high voltage (6.5 kV) to a sharp tungsten needle located at 1 cm distance above the surface of the sample. The discharge current has not exceeded 2 μA during the process. The poling time was varied from 40 to 60 min at the temperature in the range of 150–200 °C. In the applied poling process, a polymer sample on a glass substrate was first heated to a desirable temperature, then the high voltage was applied, and, finally, the sample was cooled to room temperature while the external electric field still switched on. In accordance to the procedure, the dipole moments within the sample were aligned under the applied field and then frozen at temperature below T_g.

NLO properties of APUs samples have been studied by second harmonic generation technique using incident light from a pulsed Nd^{3+}: YAG laser (λ = 1064 nm, pulse duration 15 ns, and light power density on the sample surface 10 kW/cm^2). The intensity of the second harmonic was measured using an automated spectrophotometer and a flat (X-cut) α-quartz sample as a standard.

3. Results and discussion

Synthesis of chromophores was accomplished by diazotization reaction of appropriate diamines (**DA-I**–**DA-VI**) followed by

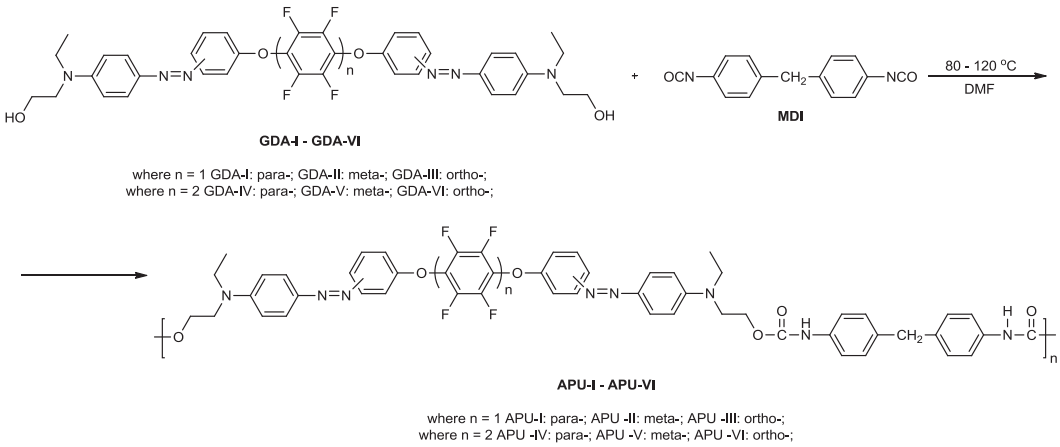

Fig. 5. Synthesis of NLO main-chain core-fluorinated azo-polyurethanes (**APU-I**–**APU-VI**).

coupling of the obtained diazonium salts (**DS-I**–**DS-VI**) with 2-[ethyl (phenyl) amino]-ethanol (Fig. 1).

The progressing of the coupling reaction of diazonium salts (**DS-I**–**DS-VI**) with the azo-component can be monitored by disappearance of the band corresponding to NH_2-group protons in ^1H NMR spectra of **GDA-I**–**GDA-VI**, which could be observed in the initial diamine compounds (**DA-I**–**DA-VI**), and by appearance of signals corresponding to hydroxyl protons (4.79–4.83 ppm), methylene (3.58–3.51 ppm) and methyl (1.11–1.15 ppm) groups (Fig. 2).

^{19}F NMR spectra of **GDA-I**–**GDA-III** contain one singlet of four equivalent fluorine atoms in TFB fragment, whereas the spectra **GDA-IV**–**GDA-VI** contains two doublets corresponding to four fluorine atoms in the *meta*- and *ortho*-positions to the OBF fragment.

Infra-red spectra of the synthesized monomers show broad absorption bands in the range of 3292–3400 cm^{-1}, which correspond to hydroxylic groups. The presence of methyl and methylene groups can be confirmed by the observed bands in the range 2952–2972, 2862–2882, and 2926 cm^{-1}, respectively. Perfluorinated fragments have a signature in the IR spectra in the range 1000–1010 cm^{-1} (Fig. 3).

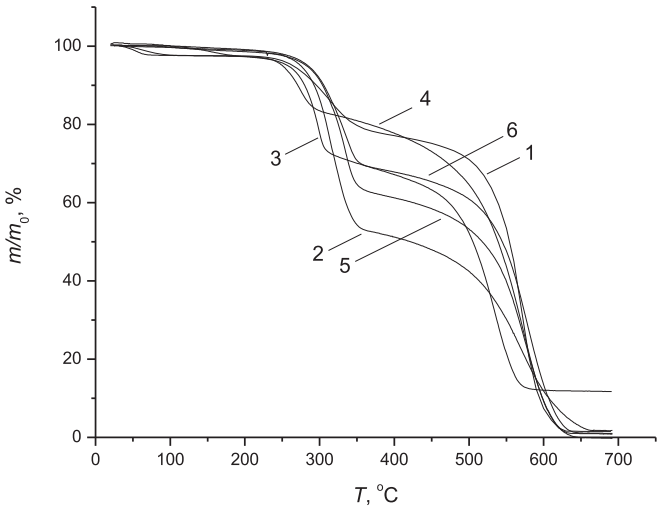

Fig. 7. Thermogravimetric curves of synthesized polyurethanes: **APU-I** (1); **APU-II** (2); **APU-III** (3); **APU-IV** (4); **APU-V** (5); **APU-VI** (6).

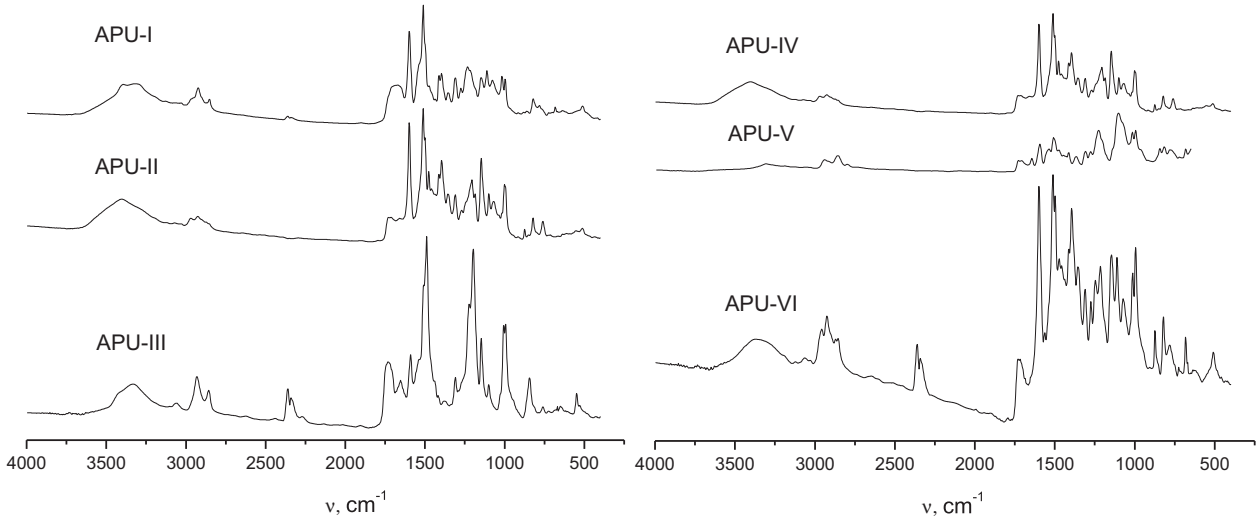

Fig. 6. IR spectra of core-fluorinated isomer forms of polyurethanes **APU-I**–**APU-VI**.

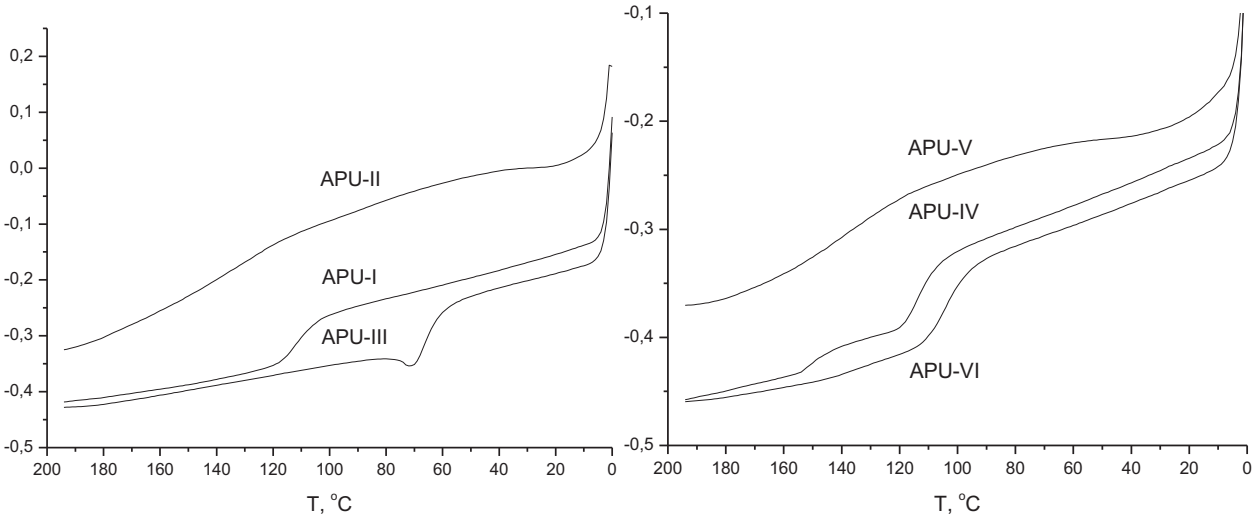

Fig. 8. DSC thermograms of fluorinated polymers **APU-I** – **APU-VI**.

On UV spectra of **GDA-I**–**GDA-VI**, the absorption maximum (λ_{max}) is observed at 418–442 nm, which corresponds to π–π^* electron transitions in *trans*-form azobenzene chromophore units (Fig. 4).

Synthesized products (**GDA-I**–**GDA-VI**) are colored powders with a good solubility in DMFA, dimethylacetamide, dimethylsulfoxide and dioxane.

By reacting hydroxyethylated diamines (**GDA-I**–**GDA-VI**), containing TFB or OBF fragments in the structure, with 4,4′-diphenylmethane diisocyanate (MDI), PUs with azo-groups in the backbone were obtained (**APU-I**–**APU-VI**) (Fig. 5).

The synthesized polymers are colored powders with a good solubility in DMFA and dimethylacetamide. Therefore, thin uniform films of the polymers were spin-cast for further optical characterization.

IR spectra of the synthesized **APU-I**–**APU-VI** have a broad band at 3300 cm^{-1} characteristic of valence vibrations of NH urethane groups as well as so-called "amide I" band at 1730 cm^{-1} as a typical signature of the carbonyl group (Fig. 6). For the most of the polymers under study, the characteristic "amide II" NH deformation band could not be identified due to its overlap with the benzene ring vibration band. All studied APUs possess an intensive band at 1150 cm^{-1}, which can be assigned to anti-symmetric stretching vibrations of C–O–C bonds within the urethane group. Also, symmetric and anti-symmetric stretching vibrations of CH in methyl and methylene groups can be found at 2962, 2872, 2926, and 2853 cm^{-1}. CF bound vibrations appear as two intensive bands in the range 1000–1010 cm^{-1} on IR spectra (Fig. 6).

Thermogravimetric analysis reveals that all the polymers under study are characterized by a two-step weight loss under heating (Fig. 7). The phenomenon was reported to be common for azo-containing polymers [42]. The first step, corresponding to the weight reduction, occurs in the range 260–295 °C and is assigned to thermal decomposition of urethane and azo-groups. The second degradation stage, a more rapid one, takes place above 500 °C and is due to both decomposition of the ester group bonds and scission of the polymer backbone.

According to the DSC results, polymer compounds under study have an amorphous structure (Fig. 8). Only glass transitions are observed, which appear as steps on the DSC scans at 112 °C, 116 °C, 66 °C and 114 °C, 141 °C, 104 °C for **APU-I** to **APU-III** and **APU-IV** to **APU-VI** correspondingly. These data show explicitly that introduction of the isomeric fragments into the polymer backbone affects significantly their glass transitions. Regardless on the fluoro component, the highest T_g can be found for polymers having azo-groups in *metha*-position (**APU-II** and **APU-V**) and the lowest ones for the polymers with azo-groups in *ortho*-position (**APU-III** and **APU-VI**). An increase in T_g with the number of fluorine atoms on going from phenylene-type to biphenyl electron-acceptor aromatic fragments should also be noted. Thus, **APU-IV**, which contains OFB aromatic part, has higher T_g in comparison with **APU-I** with less bulky TFB fragments. Similar trend can be observed

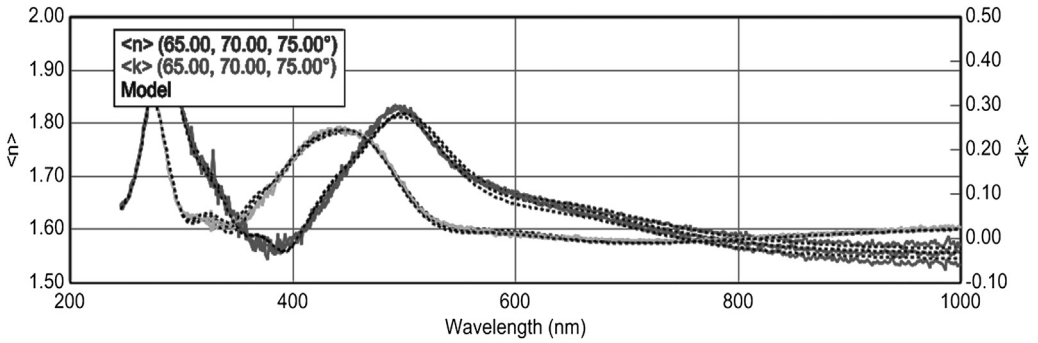

Fig. 9. An example of dispersion curves determined for **APU-II** from spectroscopic ellipsometry data at three incident angles 65, 70, and 75°. $<n>$ and $<k>$ are real and imaginary parts of the complex refractive index, respectively.

Table 1
Optical characteristics of core-fluorinated **APU-I**–**APU-VI**.

Sample	$\lambda_{max.}$, nm	k	α (10^4 cm^{-1})	n ($\lambda_{max.}$)	ε	$n_{max.}$ (at λ nm)	n (600 nm)	n (800 nm)	n (1000 nm)
APU-I	425	0.40	1.18	1.63	2.66	1.92 (490)	1.63	1.55	1.55
APU-II	440	0.24	0.69	1.66	2.76	1.82 (500)	1.67	1.58	1.55
APU-III	435	0.32	0.92	1.63	2.66	1.85 (510)	1.65	1.56	1.55
APU-IV	430	0.38	1.11	1.67	2.79	1.91 (475)	1.68	1.62	1.60
APU-V	445	0.30	0.85	1.62	2.62	1.84 (490)	1.55	1.55	1.48
APU-VI	440	0.55	1.57	1.60	2.56	2.0 (490)	1.65	1.60	1.61

comparing **APU-V** versus **APU-II**, and **APU-VII** versus **APU-III** pairs with the same isomeric substitution.

Based on our DCS results as well as literature data [43,44], we can predict that the polymers under study should have stable nonlinear optical properties (particularly, second harmonic generation coefficient) within the range of temperatures not exceeding their T_g.

Ellipsometry is as a relatively simple technique to measure optical parameters of polymer films such as film thickness (d), refractive index (n), and extinction coefficient (k). In our case, the values of $n(\lambda)$ and $k(\lambda)$ were found from spectroscopic ellipsometry data, simulating light reflection in a three-layer model: glass substrate/polymer film/air (see Fig. 9 and Table 1). As follows from the data, the absorption maximum can be found in the range of 425–445 nm for the APU polymers under study. The observed bathochromic shift of the absorption maxima in comparison to corresponding monomer chromophores corresponds to π–π^* electron transitions in azobenzene fragments covalently inserted into a polymer chain.

The values of the imaginary part of the complex refractive index k were calculated to be in the range of 0.24–0.55 for the APU polymers. Then, their molar extinction coefficients could be determined using an equation $\alpha = 4\pi\, k_{max}/\lambda_{max}$.

There are two characteristic values of the refractive index depending on the wavelength, which should be mentioned in the context of our study. The refractive index goes through a maximum at a certain λ. These maximum values (n_{max} in Table 1) spread in the range of 1.82–2.0 depending on the polymer structure. There are also refractive index values corresponding to the absorption maximum $n(\lambda_{max})$. These are also relatively high and fall the range of 1.60–1.67 for APU polymers.

The dielectric constant ε can be also determined based on the ellipsometry data as the squared refractive index at zero frequency, n_1. Assuming Lorentz function for weakly interacting oscillators (chromophores), one can consider $n_1 \approx n(\lambda_{max})$ (i.e., at the wavelength of the absorption maximum) and therefore $\varepsilon \approx n^2(\lambda_{max})$.

One of the common parameters used to characterize NLO properties of polymers is their second harmonic generation coefficient d_{33} [45]. This parameter is summarized in Table 2 for polymers under study and shows that all of them have relatively high NLO activity. The only exception is polymer **APU-III** where the value of d_{33} could not be determined due to a low stability of this polymer under intensive laser beam during NLO measurements.

Table 2
NLO characteristics of APUs polymer films.

Sample	Film thickness, (μm)	d_{33}, (pm/V)
APU-I	0.35	10.0
APU-II	0.62	2.0
APU-III	0.33	–
APU-IV	0.17	1.0
APU-V	0.55	3.5
APU-VI	0.22	5.0

According to the data of Table 2, the highest NLO activity among the APU polymers with TFB fragments in their chromophores is observed for **APU-I** (d_{33} = 10.0 pm/V) – i.e., a polymer based on **GDA-I** unit with azo-groups in *para*-position. Among the APUs with OFB electron-accepting groups the highest SHG coefficient was found for **APU-VI** (d_{33} = 5.0 pm/V) – i.e., for the case of azo-groups in *ortho*-position. Also, in the series of considered polymers, SHG coefficients tend to increase when going from **APU-IV** to **APU-VI** (see Table 2).

High hyperpolarizability of molecular chromophores is a necessary but not sufficient condition for macroscopic second-order NLO properties. A proper design of polymer materials with high macroscopic quadratic nonlinearity requires a non-centrosymmetric arrangement of NLO chromophores, which is typically achieved by means of the poling process as described above. Naturally, the stability of the induced alignment of chromophores depends on the polymer T_g and the strength of dipole–dipole interactions of the chromophore fragments. Post-poling relaxation (disorientation of the of the NLO chromophores) can significantly reduce the "real" NLO properties of a polymer material [1].

In a summary, we have synthesized two sets of new core-fluorinated isomeric azo-containing bis-diols of V-type with TFB or OFB electron-accepting fragments.

Based on these azo-chromophores, polyurethanes were synthesized, incorporating the NLO chromophores in the polymer backbone. Our study of physical, chemical, optical and nonlinear optical properties of the synthesized polymers shows that their NLO properties are mainly dependent on the isomeric nature of the polyurethane backbone rather than on the electron-accepting properties of the azo-chromophore fragments. We demonstrate also high thermal stability of the synthesized polymers and possible variation of their SHG coefficients in the range of 1.0–10.0 pm/V by modifications of the chemical structure and isomeric form of their fluorinated fragments.

References

[1] Shevchenko VV, Sidorenko AV, Bliznyuk VN, Tkachenko IM, Shekera OV. Polym Sci Ser A 2013;55(1):1–31.
[2] Tsukruk VV, Bliznyuk VN. Prog Polym Sci 1997;22(5):1089–132.
[3] Caruso U, Casalboni M, Fort A, Fusco M, Panunzi B, Quatela A, et al. Opt Mater 2005;27(12):1800–10.
[4] Ballet W, Verbiest T, Van Beylen M, Persoons A, Samyn C. Euro Polym J 2001;37(12):2419–24.
[5] Li Z, Yu G, Li Z, Liu Y, Ye C, Qin J. Polymer 2008;49(4):901–13.
[6] Moon K-J, Shim H-K, Lee K-S. Mol Cryst Liq Cryst Sci Tech. Section A. Mol Cryst Liq Cryst 1994;247(1):91–7.
[7] Lin W, Cui Y, Gao J, Yu J, Liang T, Qian G. J Mater Chem 2012;22(18):9202–8.
[8] Woo HY, Shim H-K, Lee K-S. Macromol Chem Phys 1998;199(7):1427–33.
[9] No HJ, Jang H-N, Jin Cho Y, Lee J-Y. J Polym Sci Part A: Polym Chem 2010;48(5):1166–72.
[10] No HJ, Cho YJ, Lee J-Y. Mol Cryst Liq Cryst 2010;520(1):179/[455]–185/[461].
[11] Lee J-Y, Bang H-B, Kang T-S, Park E-J. Euro Polym J 2004;40(8):1815–22.
[12] Pan Y, Tang X, Zhu L, Huang Y. Euro Polym J 2007;43(3):1091–5.
[13] Kim T-D, Lee K-S, Jeong YH, Jo JH, Chang S. Synth Metals 2001;117(1–3):307–9.
[14] Tasaganva RG, Kariduraganavar MY, Inamdar SR. Synth Metals 2009;159(17–18):1812–9.

[15] Zhu Z, Li Q, Zeng Q, Li Z, Li Z, Qin J, et al. Dyes Pigments 2008;78(3):199–206.
[16] Li Z, Wu W, Ye C, Qin J, Li Z. J Phys Chem B 2009;113(45):14943–9.
[17] Li Z, Dong S, Yu G, Li Z, Liu Y, Ye C, et al. Polymer 2007;48(19):5520–9.
[18] Xu C, Wu B, Dalton LR, Ranon PM, Shi Y, Steier WH. Macromolecules 1992;25(24):6716–8.
[19] Li Q, Li Z, Ye C, Qin J. J Phys Chem B 2008;112(16):4928–33.
[20] Li Q, Li Z, Zeng F, Gong W, Li Z, Zhu Z, et al. J Phys Chem B 2006;111(3):508–14.
[21] Park CK, Zieba J, Zhao CF, Swedek B, Wijekoon WMKP, Prasad PN. Macromolecules 1995;28(10):3713–7.
[22] Li Z, Wu W, Yu G, Liu Y, Ye C, Qin J, et al. ACS Appl Mater Interfaces 2009;1(4):856–63.
[23] Maslianitsin IA, Shigorin VD, Shipulo GP. Chem Phys Lett 1992;194(4–6):355–8.
[24] Nosova GI, Abramov IG, Solovskaya NA, Smirnov NN, Zhukova EV, Lyskov VB, et al. Polym Sci Ser B 2011;53(1–2):73–88.
[25] Beltrani T, Bösch M, Centore R, Concilio S, Günter P, Sirigu A. Polymer 2001;42(9):4025–9.
[26] Tsutsumi N, Matsumoto O, Sakai W, Kiyotsukuri T. Macromolecules 1996;29(2):592–7.
[27] Tsutsumi N, Matsumoto O, Sakai W. Macromolecules 1997;30(16):4584–9.
[28] Song MY, Jeon B, Kim HJ, Lee J-Y. J Polym Sci Part A: Polym Chem 2013;51(2):275–81.
[29] Wu Y, Natansohn A, Rochon P. Macromolecules 2001;34(22):7822–8.
[30] Li Z, Li Z, Ca Di, Zhu Z, Li Q, Zeng Q, et al. Macromolecules 2006;39(20):6951–61.
[31] Xin Z, Sanda F, Endo T. J Polym Sci Part A: Polym Chem 2001;39(15):2620–4.
[32] Boogers JAF, Klaase PTA, de Vlieger JJ, Tinnemans AHA. Macromolecules 1994;27(1):205–9.
[33] Pizzoferrato R, Sarcinelli F, Angeloni M, Casalboni M, Bertinelli F, Costa-Bizzarri P, et al. Chem Phys Lett 2001;343(3–4):205–11.
[34] Lanzi M, Bertinelli F, Paganin L, Costa-Bizzarri P, Cesari G. Macromol Chem Phys 2006;207(14):1253–61.
[35] Lanzi M, Paganin L. Euro Polym J 2009;45(4):1118–26.
[36] Xie H-Q, Liu Z-H, Huang X-D, Guo J-S. Euro Polym J 2001;37(3):497–505.
[37] Yakimansky AV, Nosova GI, Solovskaya NA, Smirnov NN, Plekhanov AI, Simanchuk AE, et al. Chem Phys Lett 2011;510(4–6):237–41.
[38] Li Z, Wu W, Hu P, Wu X, Yu G, Liu Y, et al. Dyes Pigments 2009;81(3):264–72.
[39] Li Z, Li P, Dong S, Zhu Z, Li Q, Zeng Q, et al. Polymer 2007;48(13):3650–7.
[40] Zeng Q, Qiu G, Ye C, Qin J, Li Z. Dyes Pigments 2010;84(3):229–36.
[41] Borodin AE, Malichenko BF. Dopov Akad Nauk Ukr RSR Ser Geol Khim Biol 1978;8:710–2.
[42] Sava I, Resmerita A-M, Lisa G, Damian V, Hurduc N. Polymer 2008;49(6):1475–82.
[43] Chen M, Dalton LR, Yu LP, Shi YQ, Steier WH. Macromolecules 1992;25(15):4032–5.
[44] Carella A, Casalboni M, Centore R, Fusco S, Noce C, Quatela A, et al. Opti Mater 2007;30(3):473–7.
[45] Chemla D, Zyss J. Nonlinear optical properties of organic molecules and crystals, vol. 1 and 2. New York: Academic Press; 1987.